

AD-A995 450

(2) ~~SECRET~~

**WT-1651-1(EX)
EXTRACTED VERSION**

OPERATION HARDTACK

Project 8.5a

Narrow-Bank Infrared Spectral Irradiance of High-Altitude Bursts

**R. Zirkind, Project Officer
Bureau of Naval Weapons
Department of the Navy
Washington, DC**



26 December 1961

NOTICE:

This is an extract of WT-1651-1, Operation HARDTACK, Project 8.5a.

**Approved for public release;
distribution is unlimited.**

**Extracted version prepared for
Director
DEFENSE NUCLEAR AGENCY
Washington, DC 20305-1000**

1 September 1985

86 11 19 035

UNCLASSIFIED

SECURITY CLASSIFICATION OF THIS PAGE

ADA 995450

REPORT DOCUMENTATION PAGE

1a. REPORT SECURITY CLASSIFICATION UNCLASSIFIED		1b. RESTRICTIVE MARKINGS	
2a. SECURITY CLASSIFICATION AUTHORITY		3. DISTRIBUTION / AVAILABILITY OF REPORT Approved for public release; distribution is unlimited.	
2b. DECLASSIFICATION / DOWNGRADING SCHEDULE			
4. PERFORMING ORGANIZATION REPORT NUMBER(S)		5. MONITORING ORGANIZATION REPORT NUMBER(S) WT-1651-1 (EX)	
6a. NAME OF PERFORMING ORGANIZATION Bureau of Naval Weapons Department of the Navy	6b. OFFICE SYMBOL (If applicable)	7a. NAME OF MONITORING ORGANIZATION Defense Atomic Support Agency	
6c. ADDRESS (City, State, and ZIP Code) Washington, DC		7b. ADDRESS (City, State, and ZIP Code) Washington, DC	
8a. NAME OF FUNDING / SPONSORING ORGANIZATION	8b. OFFICE SYMBOL (If applicable)	9. PROCUREMENT INSTRUMENT IDENTIFICATION NUMBER	
8c. ADDRESS (City, State, and ZIP Code)		10. SOURCE OF FUNDING NUMBERS	
		PROGRAM ELEMENT NO.	PROJECT NO.
		TASK NO.	WORK UNIT ACCESSION NO.
11. TITLE (Include Security Classification) OPERATION HARDTACK; PROJECT 8.5a - Narrow-Band Infrared Spectral Irradiance of High-Altitude Bursts, Extracted Version			
12. PERSONAL AUTHOR(S) R. Zirkind			
13a. TYPE OF REPORT	13b. TIME COVERED FROM TO	14. DATE OF REPORT (Year, Month, Day) 611226	15. PAGE COUNT 54
16. SUPPLEMENTARY NOTATION This report has had sensitive military information removed in order to provide an unclassified version for unlimited distribution. The work was performed by the Defense Nuclear Agency in support of the DoD Nuclear Test Personnel Review Program.			
17. COSATI CODES		18. SUBJECT TERMS (Continue on reverse if necessary and identify by block number)	
FIELD	GROUP	SUB-GROUP	
18	3	Hardtack Orange Shot Yucca Shot	
20	6	Infrared Radiation Koa Shot	
		Spectral Irradiance Teak Shot	
19. ABSTRACT (Continue on reverse if necessary and identify by block number) The objective of this project was to obtain basic data in the infrared region of approximately 1.7 to 13 microns from high-altitude nuclear detonations at an airborne station. More specifically, the objectives were to determine (1) the spectral distribution of the irradiance, particularly at late times on the order of a minute after detonation, and (2) the size and shape of the infrared fireball as a function of wavelength, in several spectral bands, and time. For correlation purposes, a megaton-range shot detonated at sea level was to be documented. In this report, the first objective is considered and the data is obtained by a rapid-scan monochromator.			
20. DISTRIBUTION / AVAILABILITY OF ABSTRACT <input checked="" type="checkbox"/> UNCLASSIFIED/UNLIMITED <input type="checkbox"/> SAME AS RPT <input type="checkbox"/> DTIC USERS		21. ABSTRACT SECURITY CLASSIFICATION UNCLASSIFIED	
22a. NAME OF RESPONSIBLE INDIVIDUAL MARK D. FLOHR		22b. TELEPHONE (Include Area Code) 202-325-7559	22c. OFFICE SYMBOL DNA/ISCM

DD FORM 1473, 84 MAR

83 APR edition may be used until exhausted
All other editions are obsolete

SECURITY CLASSIFICATION OF THIS PAGE

UNCLASSIFIED

from 1073

FOREWORD

Classified material has been removed in order to make the information available on an unclassified, open publication basis, to any interested parties. The effort to declassify this report has been accomplished specifically to support the Department of Defense Nuclear Test Personnel Review (NTPR) Program. The objective is to facilitate studies of the low levels of radiation received by some individuals during the atmospheric nuclear test program by making as much information as possible available to all interested parties.

The material which has been deleted is either currently classified as Restricted Data or Formerly Restricted Data under the provisions of the Atomic Energy Act of 1954 (as amended), or is National Security Information, or has been determined to be critical military information which could reveal system or equipment vulnerabilities and is, therefore, not appropriate for open publication.

The Defense Nuclear Agency (DNA) believes that though all classified material has been deleted, the report accurately portrays the contents of the original. DNA also believes that the deleted material is of little or no significance to studies into the amounts, or types, of radiation received by any individuals during the atmospheric nuclear test program.



UNANNOUNCED

Accession For	
NTIS CRA&I	<input checked="" type="checkbox"/>
DTIC TAB	<input checked="" type="checkbox"/>
Unannounced	<input type="checkbox"/>
Justification	
By	
Distribution/	
Availability Codes	
Dist	Avail and/or Special
A-1	

OPERATION HARDTACK — PROJECT 8.5a

NARROW-BAND INFRARED SPECTRAL IRRADIANCE OF
HIGH-ALTITUDE BURSTS

R. Zirkind, Project Officer

Bureau of Naval Weapons
Department of the Navy
Washington 25, D. C.

ABSTRACT

The objective was to measure narrow-band infrared irradiance from high-altitude nuclear detonations.

An airborne station was equipped with an infrared rapid-scan monochromator (Perkin-Elmer 108A) and a modified AN/AAS-4(XA-2) infrared mapping device. Each instrument had a single liquid-helium-cooled zinc-doped germanium detector to measure the region of about 2 to 13 microns. In this report, only the results obtained with the monochromator are discussed.

The project participated in the high-altitude shots, Teak, Orange, and Yucca, and, also, in a sea-level shot, Koa, for correlation purposes.

The magnitude of the irradiance from an Orange-like detonation represents a serious problem to equipment designed for ballistic missile early warning purposes. No results were obtained on the other three shots; however, broadband data obtained with the AN/AAS-4(XA-2) during Shots Teak, Orange, and Koa will be presented in WT-1651-2.

FOREWORD

This report presents the final results of one of the projects participating in the military-effect programs of Operation Hardtack. Overall information about this and the other military-effect projects can be obtained from ITR-1660, the "Summary Report of the Commander, Task Unit 3." This technical summary includes: (1) tables listing each detonation with its yield, type, environment, meteorological conditions, etc.; (2) maps showing shot locations; (3) discussions of results by programs; (4) summaries of objectives, procedures, results, etc., for all projects; and (5) a listing of project reports for the military-effect programs.

PREFACE

This project owes its gratitude to several organizations for their assistance: Naval Research Laboratory, Washington, D.C.; Naval Air Special Weapons Facility, Kirtland Air Force Base, New Mexico; and Air Force Research Division, Hanscom Field, Bedford, Massachusetts.

Further, the project gives its thanks to E. Burstein and G. Picus, formerly of the Naval Research Laboratory, for their assistance in the design and construction of the infrared detectors and to the Boeing Airplane Company, Seattle, Washington, for use of their data-reduction equipment.

CONTENTS

ABSTRACT - - - - -	5
FOREWORD - - - - -	6
PREFACE - - - - -	6
CHAPTER 1 INTRODUCTION - - - - -	9
1.1 Objectives - - - - -	9
1.2 Background - - - - -	9
1.3 Theory - - - - -	9
CHAPTER 2 PROCEDURE - - - - -	11
2.1 Shot Participation - - - - -	11
2.2 Instrumentation - - - - -	11
2.3 Installation - - - - -	11
CHAPTER 3 RESULTS AND DISCUSSION - - - - -	17
3.1 Results - - - - -	17
3.2 Discussion - - - - -	17
3.2.1 Data Difficulties - - - - -	17
3.2.2 Shot Orange Results - - - - -	18
3.2.3 Systems Applications - - - - -	19
CHAPTER 4 CONCLUSIONS AND RECOMMENDATIONS - - - - -	51
4.1 Conclusions - - - - -	51
4.2 Recommendations - - - - -	51
REFERENCES - - - - -	52
TABLES	
2.1 Flight Characteristics - - - - -	12
3.1 Wavelength-Time Correlation - - - - -	20
FIGURES	
2.1 Flight pattern of P2V aircraft, Shot Yucca - - - - -	13
2.2 Flight pattern of P2V aircraft, Shot Koa - - - - -	13
2.3 Flight pattern of P2V aircraft, Shot Teak - - - - -	13
2.4 Flight pattern of P2V aircraft, Shot Orange - - - - -	13
2.5 Monochromator assembly - - - - -	14
2.6 Zinc-doped germanium detector - - - - -	14
2.7 Spectral resolution of monochromator - - - - -	15
2.8 Schematic diagram of scan pattern - - - - -	15
2.9 Exterior view of instrumentation - - - - -	16
2.10 Schematic diagram of monochromator system - - - - -	16
3.1 Irradiance versus wavelength, for time 0 to 0.665 msec - - - - -	20

3.2 Irradiance versus wavelength, for time 2.435 to 11.665 msec-----	21
3.3 Irradiance versus wavelength, for time 13.435 to 22.535 msec-----	22
3.4 Irradiance versus wavelength, for time 24.435 to 33.535 msec-----	23
3.5 Irradiance versus wavelength, for time 35.435 to 44.535 msec-----	24
3.6 Irradiance versus wavelength, for time 46.435 to 55.599 msec-----	25
3.7 Irradiance versus wavelength, for time 57.435 to 66.535 msec-----	26
3.8 Irradiance versus wavelength, for time 68.435 to 77.599 msec-----	27
3.9 Irradiance versus wavelength, for time 79.435 to 88.662 msec-----	28
3.10 Irradiance versus wavelength, for time 90.435 to 99.662 msec-----	29
3.11 Irradiance versus wavelength, for time 101.435 to 110.535 msec-----	30
3.12 Irradiance versus wavelength, for time 112.435 to 120.662 msec-----	31
3.13 Irradiance versus wavelength, for time 123.435 to 132.662 msec-----	32
3.14 Irradiance versus wavelength, for time 134.435 to 143.662 msec-----	33
3.15 Irradiance versus wavelength, for time 145.435 to 154.662 msec-----	34
3.16 Irradiance versus wavelength, for time 156.435 to 165.599 msec-----	35
3.17 Irradiance versus wavelength, for time 167.435 to 176.662 msec-----	36
3.18 Irradiance versus wavelength, for time 178.435 to 187.535 msec-----	37
3.19 Irradiance versus wavelength, for time 189.435 to 198.599 msec-----	38
3.20 Irradiance versus wavelength, for time 200.435 to 209.599 msec-----	39
3.21 Irradiance versus wavelength, for time 211.435 to 220.662 msec-----	40
3.22 Irradiance versus wavelength, for time 222.435 to 231.599 msec-----	41
3.23 Irradiance versus wavelength, for time 233.435 to 242.662 msec-----	42
3.24 Irradiance versus wavelength, for time 244.561 to 253.662 msec-----	43
3.25 Irradiance versus wavelength, for time 255.435 to 264.662 msec-----	44
3.26 Irradiance versus wavelength, for time 266.435 to 275.599 msec-----	45
3.27 Irradiance versus wavelength, for time 277.435 to 286.662 msec-----	46
3.28 Irradiance versus wavelength, for time 288.435 to 297.599 msec-----	47
3.29 Spectral irradiance versus time, for $\lambda = 2.05$ microns-----	48
3.30 Calculated irradiance versus wavelength for $T_{BB} = 25,000^\circ K$ -----	49
3.31 Irradiance versus wavelength (of spectrum in Figure 3.2 without overlap)-----	50

Chapter 1

INTRODUCTION

1.1 OBJECTIVES

The objective was to obtain basic data in the infrared region of approximately 1.7 to 13 microns from high-altitude nuclear detonations at an airborne station.

More specifically, the objectives were to determine (1) the spectral distribution of the irradiance, particularly at late times on the order of a minute after detonation, and (2) the size and shape of the infrared fireball as a function of wavelength (in several spectral bands) and time. Finally, for correlation purposes, a megaton-range shot detonated at sea level was to be documented.

In this report, only the first objective is considered, that is, the data obtained by a rapid-scan monochromator.

1.2 BACKGROUND

Prior to Operation Hardtack, no thermal data existed beyond 2.5 microns, and the data between 0.88 and 2.5 microns was meager, since conventional instrumentation is primarily designed for the visible region of the spectrum. During Operation Redwing, spectral data was obtained in the near-infrared region (Reference 1).

Although the lead-sulfide cells used in Operation Redwing had sufficient sensitivity to record the irradiance in the 2-micron region for a considerable length of time (approximately 10 to 20 times greater than the time to second maximum, t_{\max}), the time constant of the cells was too low to obtain a time resolution better than a millisecond. In view of this limitation, instrumentation designed primarily for infrared detection, i.e., having a greater sensitivity and a faster time constant, was needed. The average sensitivity of the detectors used by this project was about 400 volts/watt in the region of 2 to 13 microns; the time constant was less than 10^{-9} second.

The military significance of the data is the accumulation of background information necessary to evaluate present and future infrared systems designed for missile detection and missile guidance. At present, the artificial background produced by Hardtack-like detonations is of vital concern to designers of ballistic missile early warning systems using infrared sensors, e.g., the Midas satellite. To produce an effective weapon system, the information as to the extent, spectral characteristics, and duration of this background is required.

1.3 THEORY

For a sea-level detonation, the thermal radiation emitted prior to shock breakaway, i.e., prior to shock-wave detachment from the fireball, can be fitted to a black-body curve whose temperature is approximately equal to the shock temperature. After breakaway, the shocked air of the fireball becomes transparent, and the spectral distribution of the emitted radiation indicates that the fireball has a color temperature.

Thereafter, the color temperature decreases monotonically. The temperature of the fireball is

yield dependent—as the yield increases the temperature decreases, since the shocked air remains opaque for a longer period of time. As the altitude increases, the shock front produced by a kiloton device becomes increasingly more transparent at early times; finally, at about 150,000 feet, the shocked air is always transparent, and there is no breakaway. The same phenomenon would occur at or above 200,000 feet for all yields (References 2 and 3).

The spectral distribution of radiation emitted by an excited source is defined if the source is in thermodynamic equilibrium. Then the spectrum will correspond to a black body emitting at the equilibrium temperature of the source. For sea-level detonations, the black-body concept is established, that is, the observed spectral emission can be fitted with the spectrum of a black body where the temperature of the shock front determines the equilibrium temperature. For high-altitude detonations, thermodynamic equilibrium is not established; consequently, the quantity of radiation emitted in the intermediate infrared region of 2 to 12 microns cannot be readily estimated. For example, shock-tube measurements indicate that nitric oxide (NO) overshoots its equilibrium value (Reference 4).

The assumption of thermodynamic equilibrium is not valid at early times, especially for all the molecular species created. Also, the air beyond the visible fireball which is excited by X- and gamma radiation can fluoresce in the infrared and produce an infrared fireball considerably larger than the visible one.

An estimate of the spectral distribution of the infrared radiation emitted by a high-altitude shot is most difficult: the kinetics of many possible molecular reactions are unknown, as are the wavelength and intensity of the spectral bands. Qualitatively, at early times (in the order of milliseconds), the highly excited nitrogen and oxygen molecules, molecular ions, free-free transitions or bremsstrahlung (the transition an electron makes between two of its free states in the presence of a force center), and nitrogen oxides can emit most intensely. As time proceeds, the atmospheric gases emit or absorb, along with the other reaction products. Thus, similar species can be expected in the aurora, such as N_2^+ , NO, NO_2 , N_2O , N_2 , O_2 , N, and O_3 , plus a host of others that can probably be formed by the high temperature associated with the explosion. In the region of 1 to 3 microns, electron transitions can be expected, whereas at the longer wavelengths vibration-rotation transitions should predominate.

Chapter 2

PROCEDURE

2.1 SHOT PARTICIPATION

This project participated in Shots Teak, Orange, Yucca, and Koa. The first three were to obtain data on high-altitude shots, and the last was for correlation purposes.

The aircraft (P2V-5F) flight plan for each event is shown in Figures 2.1 through 2.4. In each event, the radial distance between the point of detonation and the aircraft was held constant during the period of data recording. The pertinent details of each flight are given in Table 2.1. It should be noted that the data for Teak and Orange is based on the shot positions given in Reference 5.

2.2 INSTRUMENTATION

The instrument used to obtain the spectral irradiance was a Perkin-Elmer 108A f/4.5 double-pass rapid-scan monochromator. Reference 6 gives a detailed description of this monochromator.

The sensor employed was a zinc-doped germanium 1- by 6-mm crystal cooled to liquid-helium temperature, 40° K. Figures 2.5 and 2.6 are photographs of the monochromator and detector, respectively.

The monochromator used a NaCl 60° prism and scanned at the rate of 90 spectra/sec. The entrance slit was set at maximum value, 2 mm, with the resultant spectral resolution shown in Figure 2.7.

The instrument was set to scan between about 1.7 and 13 microns. A germanium filter at the entrance slit served as a cutoff at about 1.7 microns and a BaF₂ filter on the detector limited the upper end to about 13.5 microns. The internal chopper determined the actual limits of the spectral band, 1.7 to 13.02 microns.

As time increases, the spectral band is scanned, for instance, from 1.7 to 13.02 microns; the chopper then interrupts the beam, with the result that no radiation passes through the monochromator for 16 percent of the scan cycle. The scan mirror then reverses its motion and produces a mirror image—namely, scans from 13.02 to 1.7 microns, etc. The mode of scanning is schematically shown in Figure 2.8.

The detailed calibration and responsivity of the system is described in Reference 6. Because the detector is primarily for long wavelengths (Reference 7), the sensitivity improves with wavelength, that is, at 1.7 microns the response is 2 volts/watt whereas at 10 microns it is 340 volts/watt.

2.3 INSTALLATION

The monochromator was installed in a P2V-5F Navy aircraft. The instrument mount was aligned with the longitudinal axis of the aircraft and was capable of manual rotation about the polar plane. An optical ringsight was boresighted with the entrance slit, to provide an alignment reference for the operator. This combination permitted accuracy of tracking the center of the detonation to a fraction of a degree. An exterior view of the installation is shown in Figure 2.9.

The signal from the detector preamplifier was fed to a dual three-channel Philbrick amplifier. Each of the three channels provided gains of 10, 33, and 100, respectively. The output of one set of three amplifiers was passed through the FM record system of an Ampex 814 airborne recorder; the output of the other set was passed through an AM record system.

In addition, the signals from (1) a precision 240-cps oscillator and (2) a bluebox were recorded on the FM part of the Ampex tape recorder. The bluebox was used only during Shots Koa, Teak, and Orange, and its mode of operation was to act at time zones as an on-switch to the spectral reference signal produced by a synchronous generator within the monochromator. The schematic arrangement of the monochromator system is shown in Figure 2.10. The blank channel was used to separate the FM from the AM channels to prevent crosstalk.

TABLE 2.1 FLIGHT CHARACTERISTICS

Shot	Shot	Aircraft	Horizontal Range	Bearing		True
	Altitude	Altitude		From Aircraft	Heading	
	ft	ft	ft	deg	min	deg
Yucca		22,000	90,489 = 2 pct	062	—	159
Koa	0	9,100	127,365	269	35	350
Teak	250,380	21,920	287,200 = 2 pct	180	—	266.5
Orange	140,990	22,000	389,500 = 1 pct	178	30	271.50

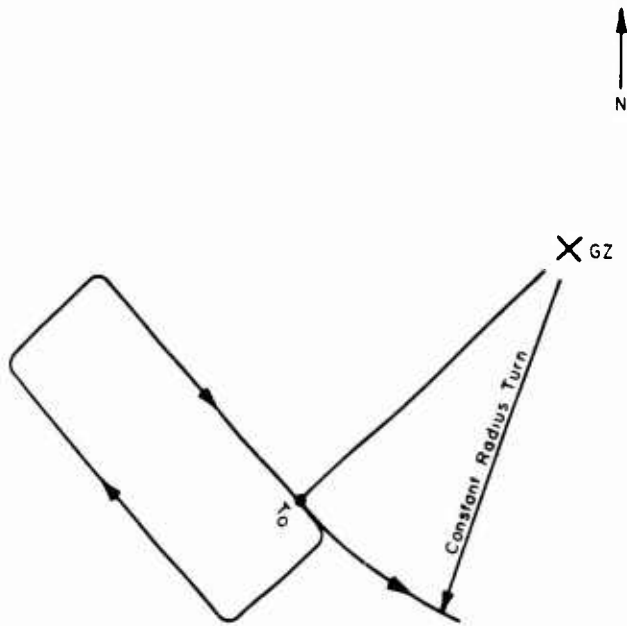


Figure 2.1 Flight pattern of P2V aircraft, Shot Yucca.

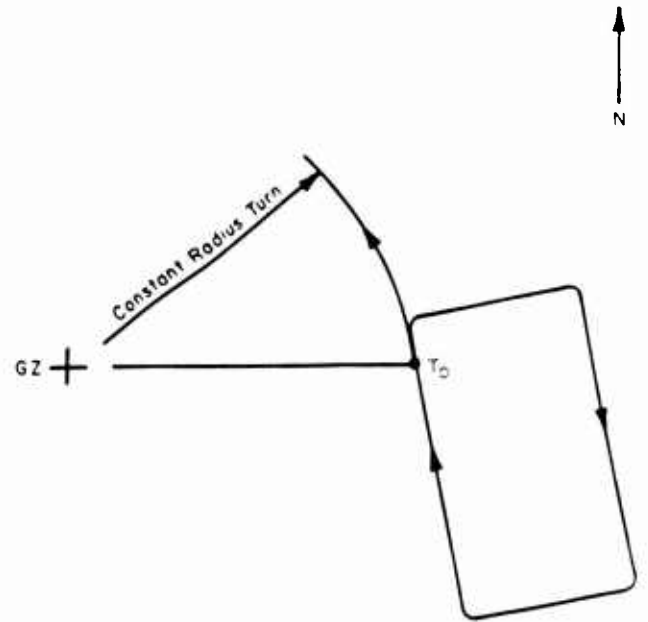


Figure 2.2 Flight pattern of P2V aircraft, Shot Koa.

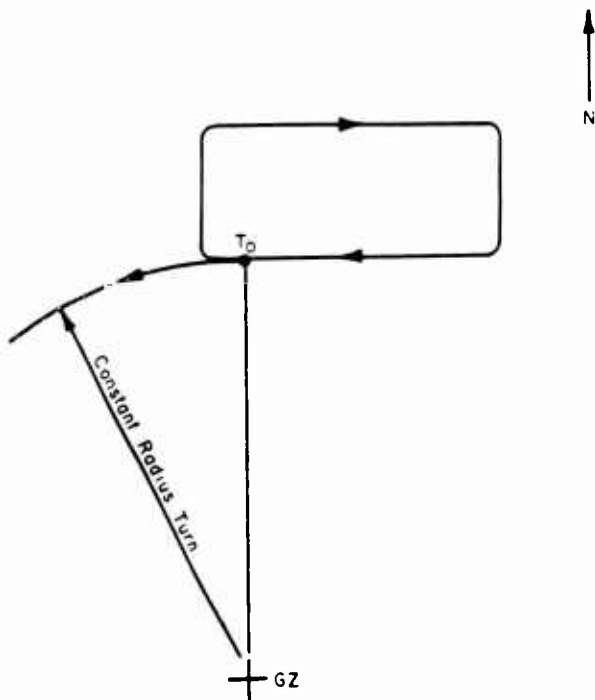


Figure 2.3 Flight pattern of P2V aircraft, Shot Teak.

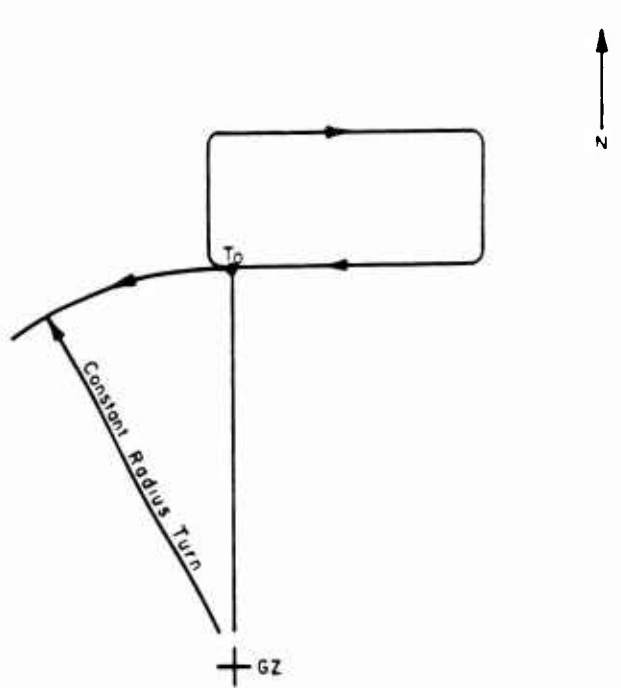


Figure 2.4 Flight pattern of P2V aircraft, Shot Orange.

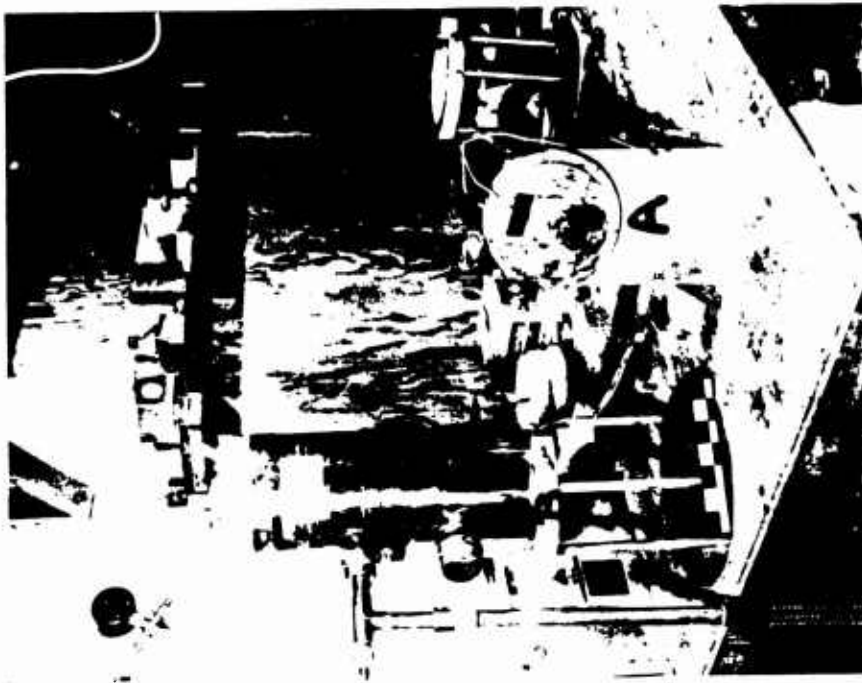


Figure 2.6 Zinc-doped germanium detector:
(A) bottom view and (B) side view.

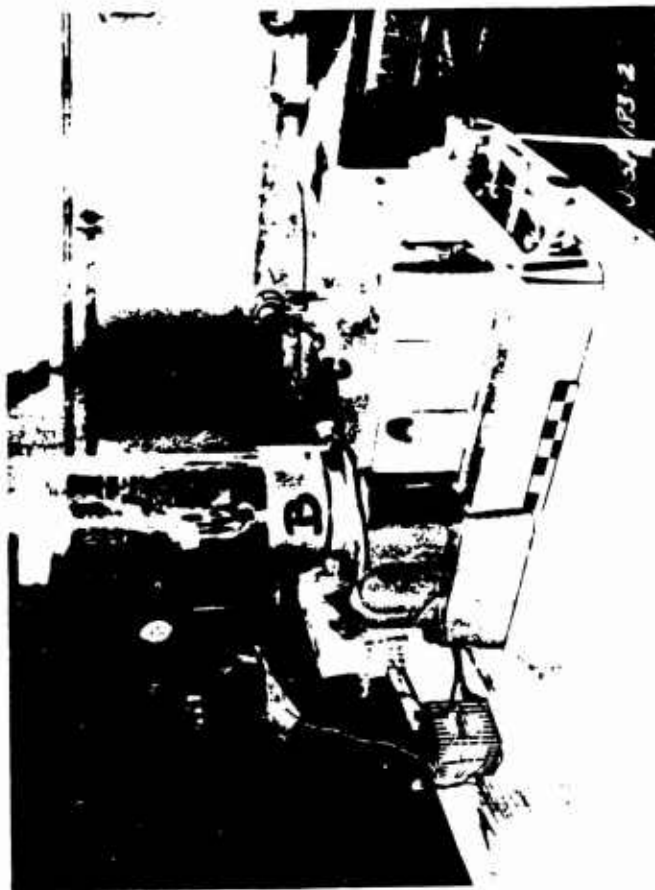


Figure 2.5 Monochromator assembly: (A) germanium filter,
(B) detector, and (C) sight.

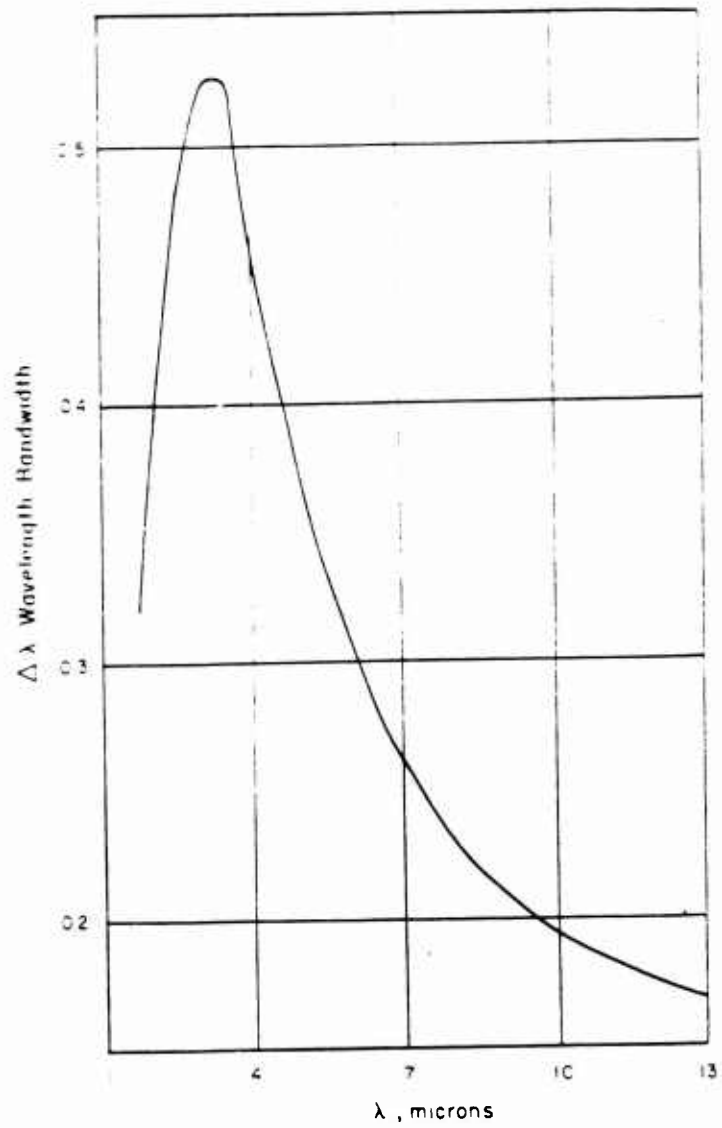


Figure 2.7 Spectral resolution of monochromator.

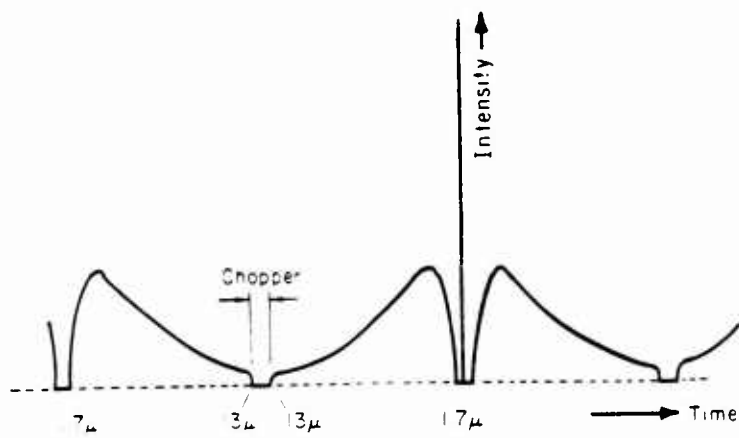


Figure 2.6 Schematic diagram of scan pattern.

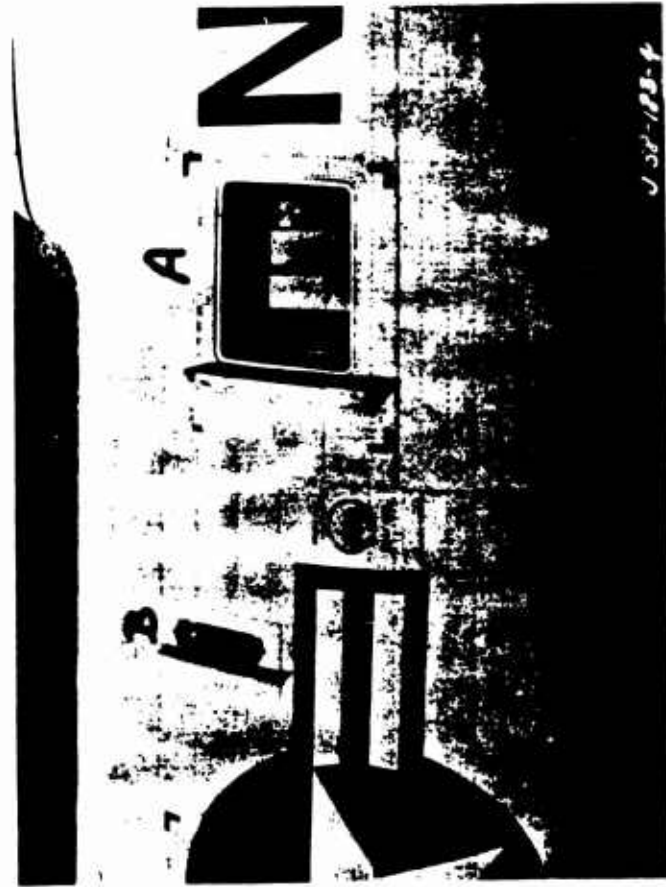


Figure 2.9 Exterior view of instrumentation: (A) AN/AAS-4 and (B) monochromator.

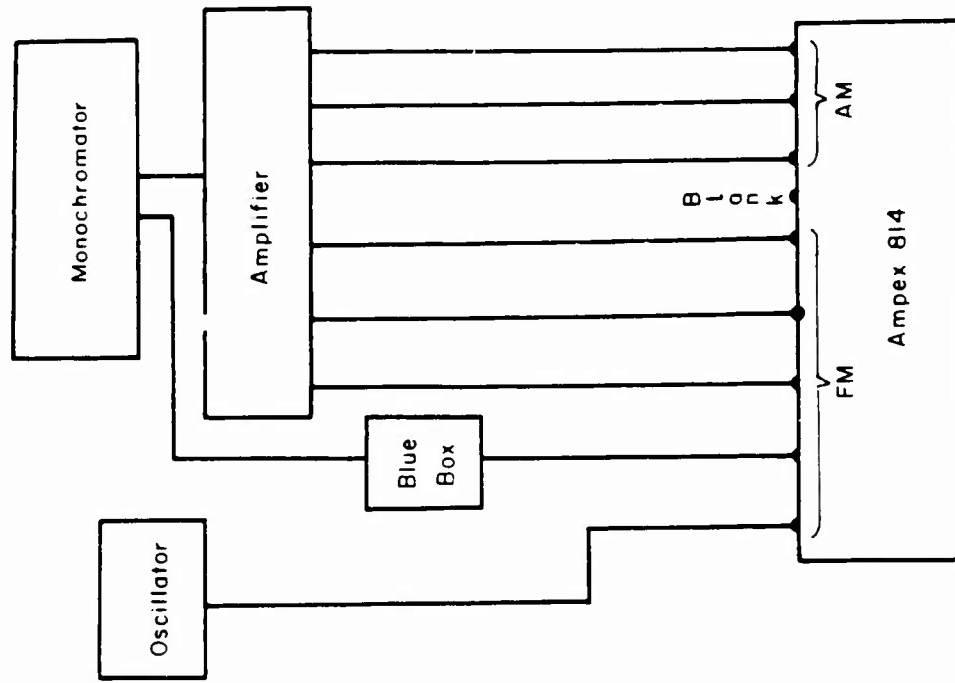


Figure 2.10 Schematic diagram of monochromator system.

Chapter 3

RESULTS AND DISCUSSION

3.1 RESULTS

The only results obtained with the rapid-scan monochromator were for Shot Orange

No data was obtained from the other shots for the following reasons: (1) Koa and Yucca were energy-limited at the monochromator and (2) Teak was outside the instrument's field of view.

The analog results obtained for Orange were converted to irradiances, i.e., watts/cm² at the measuring station versus wavelength, and are presented graphically in Figures 3.1 through 3.28. In addition a second abscissa is added, namely, time in msec. In view of the scan system described earlier (Section 2.2), there is a direct relation between wavelength and time. The relationship is presented in Table 3.1: to find the time corresponding to a particular wavelength in any figure, add the number in the table to the initial digit shown in Figures 3.1 through 3.28.

The observed minimum detectable signal is approximately 10⁻⁶ watt/cm² at a signal-to-noise ratio of 3. This is in agreement with a theoretical estimate of the system. Hence, in the event an absorption band had a minimum at less than 10⁻⁶ watt, this minimum would not be observed.

The accuracy of the irradiance is ± 10 percent. The application of the experimental error to the results in Figures 3.1 through 3.28 can eliminate some minor irregularities in the spectral curves.

With regard to the wavelength, the accuracy is 0.04 μ for the regions of 2.0 μ to 7.0 μ and 1.7 μ to 2.0 μ; accuracy is 0.09 μ for the region of 7.0 μ to 13.02 μ.

3.2 DISCUSSION

The primary objective of this project was to obtain infrared data from the two high-altitude shots, Teak and Orange, and secondarily, from Yucca and a sea-level shot. Since monochromator data was obtained for Shot Orange only, the objective of the project was only partially met with this instrument. However, broadband spectral data was obtained for Teak, Orange, and Koa with the modified AN/AAS-4(XA-2) and will be reported on in WT-1651-2 (Reference 8).

3.2.1 Data Difficulties. The failure to obtain data on three of the shots can be readily explained. In the case of Teak, the point of detonation was about 8° off axis relative to the optical axis of the monochromator; therefore, the irradiance level was too low to be recorded. The participation in Yucca was marginal because the normal daytime sky background is 50 to 500 microwatts/cm²/sterad/micron.

In the case of Koa, the irradiance may have been below the detectable limit for the monochromator. To substantiate this point, an estimate is now presented.

If it is now assumed that the spectral energy partition is directly proportional to the yield, then 6.4 × 10⁻⁶ watt/cm² is expected for the 1.10-Mt Koa Shot. (The yield for Koa is taken to be 1.10 Mt for these calculations. Later information indicates

a better yield is 1.31 = 0.08 Mt.) This spectral irradiance for Koa is obtained by applying the necessary corrections to the former measured value,

$$H_{\lambda}(\text{Koa}) = H_{\lambda_1} \left(\frac{W}{W_1} \right) \left(\frac{R_1}{R} \right)^2 \left(\frac{T}{T_1} \right) \left(\frac{\theta}{\theta_1} \right)^2 \left(\frac{\Delta \lambda}{\Delta \lambda_1} \right) \quad (3.1)$$

Where: W, R, T, θ , and $\Delta \lambda$ are yield, range, transmission, field of view, and spectral bandwidth.

After substitution of the appropriate values,

$$H_{\lambda}(\text{Koa}) = 4 \times 10^{-4} \left(\frac{1.1}{0.365} \right) \left(\frac{6.9}{22} \right)^2 \left(\frac{0.10}{0.96} \right) \left(\frac{10}{18} \right)^2 \left(\frac{0.45}{0.28} \right) \approx 6.4 \times 10^{-6} \frac{\text{watt}}{\text{cm}^2} \quad (3.2)$$

Finally, when Equation 3.2 is corrected for the cosine of the measuring station relative to the fireball disk, the expected irradiance becomes 3.2×10^{-6} watt/cm². Hence, any minor perturbations in the atmospheric transmission could reduce the irradiance below the detectable limit.

3.2.2 Shot Orange Results. The analysis of the Orange data was terminated at 300 msec, because the signal level was decreasing significantly.

The second and third spectra

in comparison to subsequent spectra clearly indicate that the latter time period corresponds to the time to the minimum. This is shown graphically in Figure 3.29. It should be noted that a second minimum appears — this second minimum has been observed by other investigators (Reference 9). The second peak may be due to the energy contributed to the radiating air by the device debris (Reference 1). It occurs too late in time to be caused by any nonequilibrium processes, whereas hydrodynamical calculations for Orange indicate that the debris would reach the shock front

The general characteristics of the spectra are as follows: (1) the irradiance has a marked increase 2) the irradiance at the longer wavelengths, is comparable to that for shorter wavelengths; and (3) absorption by atmospheric gases between source and receiver is not distinctive.

The sharp increase at the shorter wavelengths can be attributed to the emission from free-free transitions and N_2^+ (Reference 4). The irradiance at the longer wavelengths is not consistent with a Planckian distribution; at 13μ the irradiance should be down about a factor of 10 from the value at 9μ (Figure 3.30). A possible explanation is that the source radius is increasing with wavelength, and consequently a reduction in the inverse square attenuation could increase the value of the irradiance.

Figure 3.30 is a graph of the calculated irradiance at the measuring station as a function of wavelength (solid line). The calculation is based on Planck's law for a black body with unit emissivity at and with a spectral resolution equivalent to the monochromator system. The source radius was assumed to be 5,000 feet, that is, equivalent to the observed visible fireball radius. In addition, the absorptions by atmospheric gases, H_2O and O_3 and CO_2 , are superimposed along with the effect of the free-free transitions. The atmospheric transmission was calculated by the procedure in Reference 10. Some possible emission and absorption band values for different molecular species are also shown in Figure 3.30.

A comparison between Figure 3.30 and the curves in Figures 3.1 through 3.28 indicates that in most instances the effect of atmospheric absorption is nonexistent. To illustrate this point, Figure 3.6 was corrected for atmospheric absorption, with the result that the spectral distribution is dominated by the prominences at the wavelengths corresponding to the absorption bands

of H₂O and CO₂. A more typical distribution exhibiting atmospheric absorption is Figure 3.4.

A possible explanation is that the emission from known and unknown species, including H₂O, O₃, and CO₂, is sufficient to override at times the absorption by the atmosphere. When these gases emit, the wavelength of the emission band is at a somewhat longer wavelength than the absorption band. In addition, under the environmental conditions of a nuclear detonation (high pressure and temperature), the bands are broadened. For example, nitric oxide (NO) can absorb at about 2.7 μ , but when excited in a shock tube it can emit from 2.8 μ to 3.3 μ . A more detailed analysis can be made if the source radii as a function of wavelength and time and the broadband spectral data obtained with the AN/AAS-4 are available.

The results in Figures 3.1 through 3.28 contain the nonlinear effect of the prism dispersion, that is, the resolution decreases from 1.7 μ to 3 μ and then increases from 4 μ to 13 μ . This effect would have the tendency to increase the irradiance levels in the region of 2 to 5 microns, and minimize any absorption bands.

The irradiance as a function of wavelength for discrete but contiguous bands was constructed and is shown in Figure 3.31. This curve again shows no distinct features except for emphasizing the large amount of radiation emitted at wavelengths less than 2 μ . The spectral distribution obtained in a shock tube for air at a temperature of 8,000° K is shown for comparison.

Chapter 4

CONCLUSIONS AND RECOMMENDATIONS

4.1 CONCLUSIONS

For high-altitude detonations like Orange, thermodynamic equilibrium is not established at early times of less than 1 second. The spectral distribution indicates that emissions occur intermittently at the wavelength regions corresponding to the absorption bands of the atmospheric gases to override the absorption.

The scattered infrared radiation from Shot Teak was below the detectable level of the monochromator (10^{-6} watt/cm²).

It may be inferred from the lack of results that the quantity of infrared radiation available from a Yucca-like shot is insufficient to be militarily significant.

4.2 RECOMMENDATIONS

In the event of any future high-altitude shots, infrared measurements at wavelengths greater than 1 micron should be made. The instrumentation should have a higher spectral and time resolution, and should include pre-slit optics.

REFERENCES

1. R. Zirkind; "Airborne High-Resolution Spectral Analysis" (U); Project 8.5, Operation Redwing, WT-1342, July 1960; Bureau of Aeronautics, Department of the Navy, Washington, D. C.; Secret Restricted Data.
2. H. L. Brode and F. R. Gilmore; "Estimates of the Thermal Radiation from Nuclear Weapons Burst at High Altitudes"; RM-1983, September 1957; The RAND Corporation, Santa Monica, California; Secret Restricted Data.
3. H. L. Brode and R. E. Meyerott; "Thermal Radiation from Atomic Detonations at Times Near Breakaway"; RM-1851, August 1956; The RAND Corporation, Santa Monica, California; Secret Restricted Data.
4. "Re-entry Physics Program Semi-Annual Technical Summary Report"; Avco-Everett Research Lab. Report AERL 59-173, December 1959; Avco Corporation, Everett, Massachusetts; Secret.
5. G. P. Elliot et al; "Operation of Missile Carrier for Very-High-Altitude Nuclear Detonations" (U); Project 9.3a, Operation Hardtack, WT-1657, May 1959; U. S. Army Ballistic Missile Agency, Redstone Arsenal, Alabama; Secret Restricted Data.
6. Rapid Scan Monochromator Model 108 Instruction Manual; January 1956; Perkin-Elmer Corporation, Norwalk, Connecticut; Unclassified.
7. R. Zirkind; "A Long Wavelength Infra-red Spectrometer System"; RRSY-60-37, April 1960; Bureau of Naval Weapons, Washington, D. C.; Unclassified.
8. R. Zirkind; "Narrow-Band Infrared Spectral Irradiance of Very-High-Altitude Bursts"; Project 8.5b, Operation Hardtack, WT-1651-2; Bureau of Naval Weapons, Washington, D. C.; Secret Restricted Data.
9. R. M. Brubaker et al; "Thermal Radiation From High-Altitude Bursts" (U); Project 8.2, Operation Hardtack, WT-1648; Air Force Cambridge Research Laboratories, L. G. Hanscom Field, Bedford, Massachusetts; Secret Restricted Data.
10. T. Altshuler; "A Procedure for Calculation of Atmospheric Transmission of Infrared"; RS7ELC15, May 1957; General Electric Company Advanced Electronics Center, Ithaca, New York; Unclassified.